The electrometer concept and binding of cations to phospholipid bilayers

Andrea Catte,[*] Mykhailo Girych,[†] Matti Javanainen,[‡] Markus S. Miettinen,[§] Luca Monticelli,[¶] Jukka Määttä,[**] Vasily S. Oganesyan,[††] and O. H. Samuli Ollila[‡‡]

Despite of vast amount of experimental and theoretical studies, the binding affinity of cations, especially the biologically relevant Na^+ and Ca^{2+} ions, into a phosholipid bilayer is not agreed on in the literature. Here we directly compare the measured choline headgroup order parameters to the simulations with different models in the presence of different cations. We conclude that the simplest explanation for the experimental and theoretical observations is that at mM concentrations the Na^+ ions do not ~~penetrate into~~ bind to **1.Markus: 'penetrate into' gives the impression they go really deep, that is, even in the tails. On the other hand, 'bind to' could mean that they are bound just to the headgroup region. Should we maybe say precisely until where do they penetrate?** phosphatidylcholine lipid bilayers, in contrast to Ca^{2+}. Further, the binding affinity of Na^+ is overestimated in almost all molecular dynamics simulation models. However, the electrometer concept (connecting the choline order parameter changes to the amount of penetrating charge) is valid also in simulations.

This work has been, and continues to be, progressed and discussed through the blog: nmrlipids.blogspot.fi. Everyone is invited to join the discussion and make contributions through the blog. The manuscript will be eventually submitted to an appropriate scientific journal. Everyone who has contributed to the work through the blog will be offered coauthorship. For more details see: nmrlipids.blogspot.fi.

I. INTRODUCTION

The cation interactions with phospholipid membranes occur in a large amount of physiological processes, nerve cell signalling being the prime example. Thus, the interactions between different cations and phospholipid bilayers have been very widely studied experimentally and theoretically. While it is practically agreed that the relative binding affinity of different ions follows the Hofmeister series [1–9], the quantitative binding affinities of different ions are not agreed on in the literature. The extensive reviews of the work done prior 1990 [2, 3] concluded that monovalent cations (Li^+ being an exception) interact only weakly with phospholipid bilayers, while for multivalent ions the interactions are significant. This conclusion has been supported by further studies where the bilayer poperties have remained intact with increasing monovalent salt concentration [4, 10, 11]. On the other hand, these weak interactions of monovalent ions, especially sodium, have also been questioned in several more
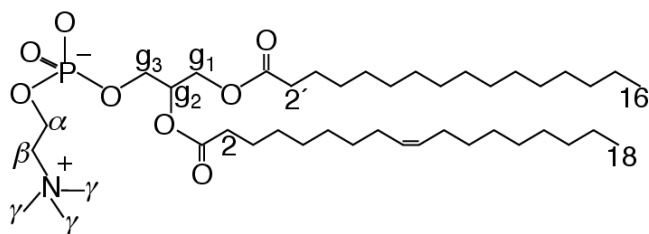

FIG. 1: Chemical structure of POPC.

recent studies suggesting stronger binding [6–9, 12–18]. In this work, we concentrate on the interactions between phospholipid bilayers and two widely studied and biologically relevant cations, monovalent sodium and divalent calcium.

One of the experimental methods used to measure ion binding is the so-called "electrometer concept" where the changes of the C–H bond order parameters for the choline α and β segments (see Fig. 1 for definitions and 1-palmitoyl-2-oleoylphosphatidylcholine (POPC) chemical structure) are used to determine the amount of penetrating charges into a bilayer [19–22]. The concept is based on the findings that the absolute value of the β order parameter increases, and the α order parameter decreases, with inceasing amount of penetrating charges [19–22]. From the simulation point of view, the electrometer concept is particularly interesting since one can directly and quantitatively compare an actual measurable set of quantities, the order parameters, to the simulations. In this work we compare the ion-induced changes in phosphatidylcholine headgroup order parameters between different simu-

---

[*] The authors are listed in alphaphetical order.; The author list is not completed.; University of East Anglia, Norwich, United Kingdom

[†] Helsinki Biophysics and Biomembrane Group, Department of Biomedical Engineering and Computational Science, Aalto University, Espoo, Finland

[‡] Tampere University of Technology, Tampere, Finland

[§] Fachbereich Physik, Freie Universität Berlin, Berlin, Germany

[¶] Institut de Biologie et Chimie des Protéines (IBCP), CNRS UMR 5086, Lyon, France

[**] Aalto University, Espoo, Finland

[††] University of East Anglia, Norwich, United Kingdom

[‡‡] **Author to whom correspondence may be addressed. E-mail: samuli.ollila@aalto.fi.**; Helsinki Biophysics and Biomembrane Group, Department of Biomedical Engineering and Computational Science, Aalto University, Espoo, Finland

lation models to resolve the above discussed controversies in the literature.

It is agreed in the literature that the Ca^{2+} ions do penetrate in the phosphatidylcholine bilayer and significantly affect membrane properties already at mM concentrations of $CaCl_2$, however, the strength of the binding is not agreed on [13, 20, 23]. **2.Markus: Mention shortly what strengths have been suggested?**

The experimental studies supporting the weak interactions between sodium ions and phospholipid bilayer have shown that at mM concentrations NaCl has a negligible effect on the choline headgroup order parameters [19], area per molecule [10], dipole potential [24], and lipid lateral diffusion [11]; in contrast, these properties are significantly affected by the presense of $CaCl_2$ or other multivalent ions. In addition, water sorption isotherm for POPC/NaCl system was essentially similar to NaCl in pure water—indicating only weak interaction between ion and lipid [4]. Only minor changes in POPC infrared spectra were observed in the presense of NaCl compared to the significant changes in the presense of $CaCl_2$ and other multivalent ions, and it was again concluded that the Na^+-lipid interactions are weak [4].

In contrast, experimentally observed decrease in fluorescent probe rotational and translational dynamics in lipid bilayer due to addition of NaCl has suggested significant ion binding also with mM concentrations [7, 9, 12]. However, the reduced lateral diffusion is not observed in NMR experiments without probes, which suggests that it arises from interactions between probe and ion, not between lipid and ion [11]. NaCl binding to phospholipids leading to the change of the strength of bilayer against rupture and area per lipid reduction has been also suggested from Atomistic Force Microscopy (AFM) [14–18]. Interpretation of calorimetric measurements has been controversial: Previously the small effect of monovalent ions (except Li^+) on phase transition temperature compared to multivalent ions was interpreted such that only multivalent ions and Li^+ specifically bind to phosholipid bilayer [2], however, more recently the small changes in calorimetric experiments have been interpreted to indicate also Na^+ binding [8, 12]. In electrophoresis measurements of phosphatidylcholine vesicles, NaCl can increase the originally negative zeta potential close to zero, however, positive zeta potential can be typically reached only with multivalent ions or Lit^+ [1, 8, 14, 15, 23]. The lack of significant positive electrophoretic mobility in the presence of NaCl has been recognized to contradict with suggested strong binding of Na^+ and the contradiction has been explained by the effect of Cl^- ions to the electrophoretic mobility [25, 26].

In atomistic resolution molecular dynamics simulations, all the generally used models seems to predict binding of Na^+ ions into a phoshatidylcholine lipid bilayer, but the strength of binding depends on model used [12, 13, 25, 27–30]. The reduction of lipid lateral diffusion due to Na^+ binding in simulations is in agreement with fluorescent probe measurements [7, 9, 12], but not with the NMR experiments [11]. The AFM experiments are interpreted to agree with the area per lipid reduction due to Na^+ binding in simulations [14–18], however, compared to the scattering experiments the area re-

duction is observed at significantly too low concentrations in simulations compared to experiments [10]. The simulations have been suggested to predict larger positive electrophoretic mobility than is experimentally measured with NaCl, which has been explained by Cl^- behaviour [25, 26].

In our recent work, we showed that the experimental order parameters for choline and glycerol backbone were not quantitatively reproduced by any available lipid model in fully hydrated conditions, however, the response of the choline order parameters to dehydration were qualitatively correct in all **3.Markus: This 'all' gives the impression that it is the same as the 'any available' in the beginning of the sentence. I propose we make it clear here that we only tested four FFs against dehydration.** models, and the response to the cholesterol content was qualitatively correct in the CHARMM36 model [31]. **4.Markus: Wouldn't you say that the response of the choline order parameters to cholesterol content was qualitatively just as correct in MacRog as it was in CHARMM36? (Fig. 9 in Ref. [31])** In this work, we show that the qualitative response of order parameters to penetrating cations is qualitatively correct, but the partitioning of ions is too strong in all the studied models.

II. RESULTS AND DISCUSSION

On the other hand, the presence of multivalent ions or charged amphiphiles changes the α and β order parameters in a systematic way suggesting that the amount and sign of charge penetrated into a bilayer can be measured from the changes of these parameters [19–22]. This is known as the "electrometer concept".

The core idea of the electrometer concept is that the decrease (increase) of β- and α-carbon order parameters is related to cation (anion) penetration into a lipid bilayer.

The effect of NaCl on the choline and glycerol bakcbone order parameters from experiments by Akutsu et al. [19] and various simulations are shown in Fig. 2. The simulated systems are described in the Table I and further details are given in Supplementary Information. The experimental results are shown for DPPC bilayer due to a more extensive data set [19], however, the measurements for POPC gave essentially the same results [20].

The order parameter changes for β- and α-segments are plotted in Fig. 2 in the presence of NaCl and $CaCl_2$ from experiments and different simulations. The clear decrease is seen in experiments with $CaCl_2$ compared to the negligible effect of NaCl. Interpreted in terms of the electrometer concept, the result indicates that Ca^{2+} ions significantly penetrate into PC bilayer in contrast to Na^+ [19, 20]. It should be noted that in the original experiments the absolute value of the β order parameter **increased** in the presence of cations, however, it was shown later that the β order parameter is negative [32–34], thus the value is actually **decreasing** (becoming more negative). Also in all simulation models the order parameter decrease with penetrating cations is observed indicating that the qualitative response is correct, despite of inaccuracies with varying severity in the choline and glycerol backbone structures in different models [31].

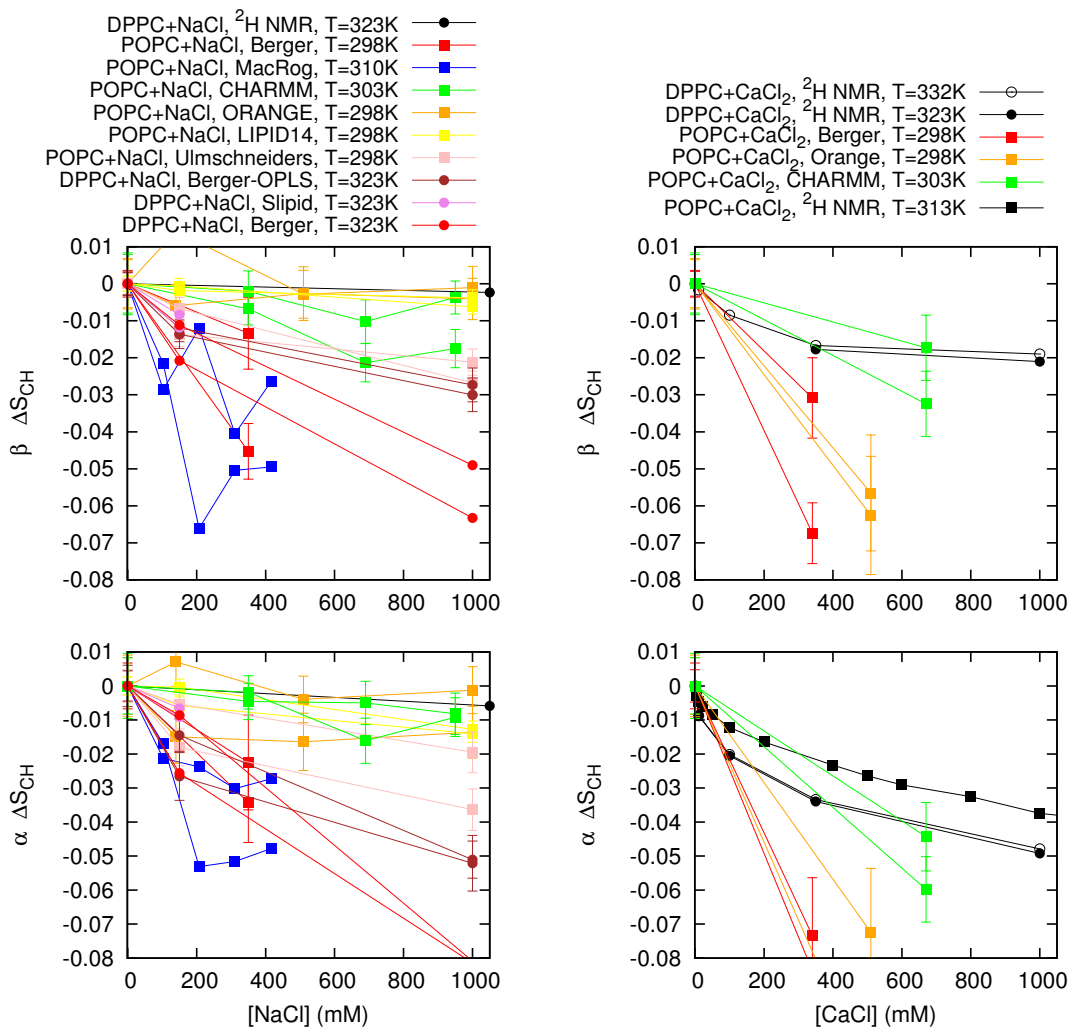To study the correlation between order parameter changes

FIG. 2: The change of order parameters for β and α segments as a function of NaCl (left column) and CaCl$_2$ (right column) concentrations from simulations and experiments by Akutsu et al. [19]. The signs of the order parameters without ions are taken from [32–34] and it is reasonable to assume that the signs do not change with concentrations represented here [20]. Note that the β order parameter with negative sign decreases here with cation penetration in contrast to measured absolute value increase in the origical studues [19, 20]. Regarding the actual electrometer concept this is not relevant, however. The experimental accuracy of order parameter changes is much higher than the accuracy of quantitative values due to high resolution of ^{2}H NMR spectroscopy [?].

5.Mykhailo Girych is already running Lipid14 and more CHARMM36 simulations with CaCl$_2$. When done those results will be added.

6.I wrote previously "I think that it would be very interesting to test the modified CHARMM ions: Venable et al. dx.doi.org/10.1021/jp401512z, J. Phys. Chem. B 2013, 117, 1018310192. According to the paper, these parameters improve the ion binding to the charged lipid bilayers. Even though I think that testing this would be highly relevant, I do not have time to do it now.". However Matti Javanainen claimed in Skype that in the current CHARMM36 simulations we already have these ions. This has to be checked.

and ion partitioning into a bilayer, suggested by the electrometer concept [19–22], the ion density distributions from different simulation models as a function of membrane normal with NaCl and CaCl$_2$ are shown in Figs. 3 and 4, respectively. The density profiles from different models in Fig. 3 are arranged to increasing order according to the changes observed in order parameters with NaCl concentration in Fig. 2 such that the model with smallest change is on top and towards the bottom are models with larger observed order parameter changes. The Fig. 2 clearly shows that the larger Na$^+$ density

peaks at the lipid bilayer interface are observed towards the bottom of the figure correlating with the increased order parameter change. Thus the Na$^+$ ion binding affinity is clearly related to the α and β order parameter changes in simulations are well, thus the electrometer concept [19–22] can be used to compare the Na$^+$ ion binding affinity between simulations are experiments. This applies to all studied models despite of the varying quality of the sampled choline and glycerol backbone structures [31]. The Ca^{2+} penetration and related order parameter decrease is seen with all simulation models.
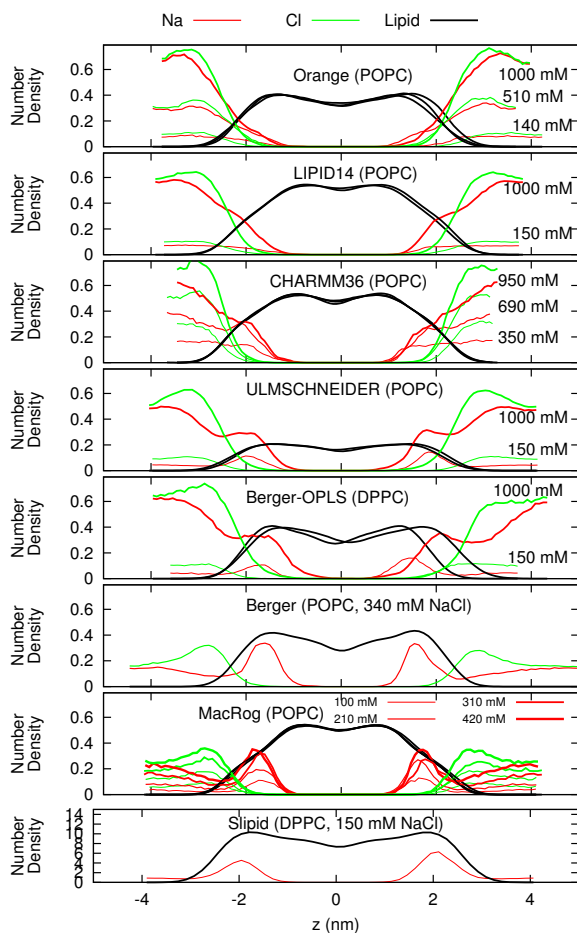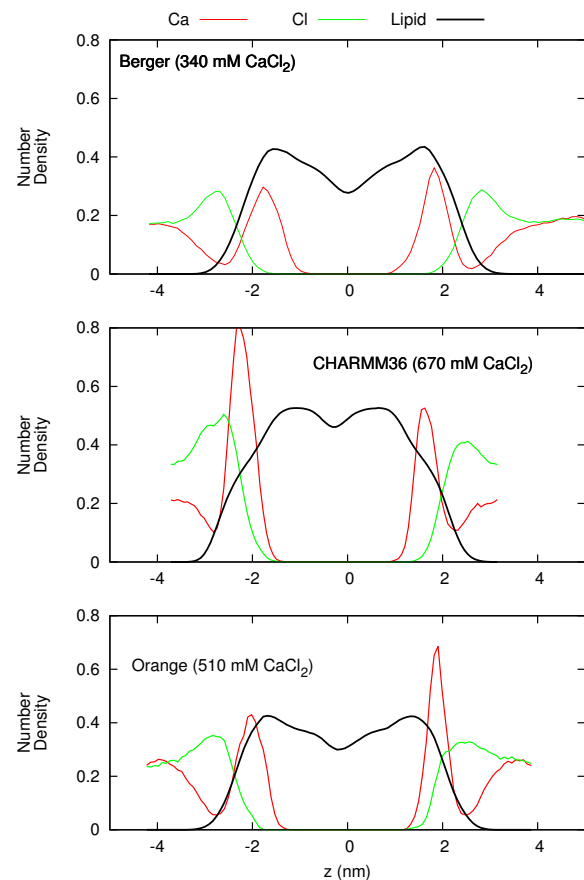
FIG. 3: Number density profiles for lipids, Na^+ and Cl^- ions from simulations with different force fields and different NaCl concetrations. The force fields are ordered according to the order parameter changes observed in Fig. 2 such that the models with smallest observed changes are top. The lipid densities are scaled with 100 (united atom) or 200 (all atom model) to make them visible with the used y-axis scale. Figure discussed in https://github.com/NMRLipids/lipid_ionINTERACTION/issues/4.

7.- For Slipids we need number densities of Na, Cl and Lipids. If data is uploaded to Zenodo, this is trivial to calculate with the current scripts.

FIG. 4: Number density profiles for lipids, Ca^{2+} and Cl^- ions from simulations with different force fields and different $CaCl_2$ concentrations. The lipid densities are scaled with 100 (united atom) or 200 (all atom model) to make them visible with the used y-axis scale. Figure discussed in https://github.com/NMRLipids/lipid_ionINTERACTION/issues/4.

8.- The CHARMM36 simulations with $CaCl_2$ is now done. With a first look it seems that the partition is similar or stronger than in Orange model even though the order parameter change was much larger in the Orange model (see Fig. 2). This would indicate that the different order parameter response in the Orange model would be due to the reaction of headgroup into penetrating charge, not due to the difference in partition. However, this requires more detailed studies. Mykhailo Girych is already running Lipid14 and more CHARMM36 simulations with $CaCl_2$. When done those results will be added.

The smallest order parameter changes in best agreement with experiments with NaCl concentration are seen for the Orange, CHARMM36 and Lipid14 models in Fig.2. However, the ion density profiles in Fig. 3 show detectable differences in Na^+ affinity between these models, Orange having lowest affinity and CHARMM36 highest. None of the models reproduces all the order parameters in Fig. 2 within experimental error and these very small order parameter changes (less than 0.02) may be delicate to, e.g. initial structures. Thus we cannot conclude if one of these three models is more realistic than another, especially with physiological NaCl concentrations ($\sim$ 150mM) which is most relevant for most applications. On the other hand, all the other studied models clearly overestimate

the choline order parameter changes respect to experiments, as seen from Fig. 2. This is related to the unrealistically strong Na^+ binding to the bilayer, evidenced by the density peaks in Fig. 3 which are seen also with physiological concentrations.

9.The discussion about $CaCl_2$ results will be written when we have all the results. Mykhailo Girych is already running Lipid14 and more CHARMM36 simulations with $CaCl_2$.

10.The ^{1}H NMR experiments suggest that the N-β-α-O dihedral is only in gaughe

conformation in the absense of ions, but in the presense of multivalent ions there would be also anti conformations present [Hauser et al. BBA 508, 450 (1978), Hauser et al. Chem. Phys. Lipids 29, 103 (1981)]. I have now calculated the dihedral distributions for this dihedral with different CaCl$_2$ concentrations in different models, see Fig. 8. The change suggested by the ^{1}H NMR experiments is not seen in the CHARMM36 model. In Orange model this dihedral is mostly in anti conformation also without CaCl$_2$, oppositely as suggested by ^{1}H NMR experiments. With CaCl$_2$ anti conformations become slightly more pronounced, however, the conformation seems to be unrealistic from the beginning so the studies of structural response to the CaCl$_2$ might not be reasonable with this model. I think we need more simulations with CHARMM36 to see how good the order parameter response to the CaCl$_2$ actually is. Then we can discuss more about its structural response. 11.The P-N vector tilting analysis should be considered

The most important observation is that the experimental order parameters for the headgroup and glycerol bakcbone g$_3$ segment 27.Markus: There seems to be NO experimental g$_3$ data in Fig. ??... are practically unhanged even though 1M NaCl concentration was added to the system. Thus, the presence of mM concentrations of NaCl does not affect the structure of these parts of lipids. ~~On the other hand, the presence of multivalent ions or charged amphiphiles changes the α and β order parameters in a systematic way suggesting that the amount and sign of charge penetrated into a bilayer can be measured from the changes of these parameters~~ [19–22]. ~~This is known as the "electrometer concept".~~ Thus, the most straightforward explanation for the experimental results shown in Fig. **??** is that the Na$^+$ and Cl$^-$ ions do not essentially penetrate into a phospholipid bilayer below 1M concentrations.

The response of order parameters to the NaCl concentration in simulations depends on the used model in Fig. **??**: The addition of NaCl leads to a significant changes for choline and g$_2$ and g$_3$ segments in glycerol bakcbone in Berger and MacRog models, while only moderate changes are seen in CHARMM36 and Orange force fields. The experimental data for glycerol backbone as a function of NaCl concentration is available only for the g$_3$ segment. 28.Markus: For some reason, these g$_3$ data are not shown in Fig. ?? The changes in g$_1$ and g$_2$ are unlikely since all the other order parameters are unaffected and ^{1}H NMR data indicates that multivalent cations binding to phospholipid interact mainly with choline group leaving glycerol backbone conformations intact [63, 64].

The most straightforward explanation for our results is that Na$^+$ ions do not practically penetrate into a PC lipid bilayer at mM concentrations, thus the presense of NaCl does not affect the bilayer properties as observed in various experiments [4, 10, 11, 19, 20, 24]. Consequently, the Na$^+$ penetration and concominant changes in order parameters, area per molecule and lateral diffusion seen in almost all simulation models would be artefact due to overestimated attraction between ions and lipid bilayer. Even though this would also explain the absense of positive zeta potential in electrophoresis experiments [1, 8, 14, 15, 23], the presented data do not rule out the suggested possibility of equal binding of Na$^+$ and Cl$^-$ ions [26], however, this equal binding should happen in such a way that the bilayer properties are unaffected. The negligible binding of Na$^+$ at mM concentrations suggested here differs from the conclusions made from measurements of fluorescent probe dynamics [7, 9, 12], membrane hardness with

AFM [14–18] and calorimetry [8, 12]. However, the fluorescent measurement results may arise from direct interactions between probe and ions, as already suggested by Filippov et al. [11]. Further, the calorimetric results have been also interpreted to support negligible binding [2], and AFM result is relatively indirect, thus there may be alternative explanations as well.

The origin for suggested inaccuracies in lipid-ion interactions in simulation models is unknown. In principle, the incorrect choline structure [31], lack of polarizability [65] or the used water model could cause such results. The effect of changes in lipid and ion models on the ion partitioning is discussed in the supplementary material. 29.In the Orange simulation only lipid model is changed, respect to Berger, and Jukka tested the effect of 0.7 charge scaling for Na ion (suggested by Leontyev et al. [65] to compensate to the lack of electronic polarizability in the model). I think we should discuss these things in supplementary material. Even though we cannot be fully conclusive, there is some essential information also in these results.

III. CONCLUSIONS

We have compared phosholipid bilayer interactions with NaCl and CaCl$_2$ between different molecular dynamics simulation models and ^{2}H NMR experiments. The comparison led to the following conclusions

- The electrometer concept suggesting connection between α and β order parameter decrease and cation partitioning [19–22] works also in simulations, despite of inaccuracies in actual atomistic resolution structures.

- The most straighforward explanation for the various experimental observations is that there is no Na$^+$ ion binding into the phospholipid bilayer at mM concentrations, in constrast to Ca^{2+} which specifically binds.

- The Na$^+$ partitioning is overestimated in almost all molecular dynamics simulation models, however, from the publicly available models the CHARMM36 has the most realistic description.

- 30.Final conclusions about the structural response to be written once we have all the results

This work has been, and will be, progressed and discussed through the blog: nmrlipids.blogspot.fi. Everyone is invited to join the discussion and make contributions through the blog. The manuscript will be eventually submitted to an appropriate scientific journal. Everyone who has contributed to the work through the blog will be offered coauthorship. For more details see: nmrlipids.blogspot.fi.

TABLE I: Simulated lipid bilayers with ions. The ion concentrations are the concentration of ions in buffer to solute the lipid bilayers and calculated as [ion]=(N_{ion}×[water])/N_w, where [water]=55.5M. These correspond the concentrations reported in the experiments by Akutsu et al. [19].

Force field	lipid	[Ion] mM	[a]N_l	[b]N_w	[c]N_{Na}	[d]N_{Ca}	[e]N_{Cl}	[f]T (K)	[g]t_{sim}(ns)	[h]t_{anal} (ns)	Files
Berger-POPC-07[35]	POPC	0	128	7290	0	0	0	298	270	240	[36]
Berger-POPC-07[35], ionFF [?]12.	POPC	340 (NaCl)	128	7202	44	0	44	298	110	50	[37]
Berger-POPC-07[35], ionFF [?]13.	POPC	340 (CaCl$_2$)	128	7157	0	44	88	298	108	58	[38]
Berger-DPPC-98[39]	DPPC	0	72	2880	0	0	0	323	?	?	[40]
Berger-DPPC-98[39], ionFF [?]	DPPC	1000 (NaCl)	72	2778	51	0	51	323	120	60	[41]
BergerOPLS-DPPC-06[42]	DPPC	0	72	2880	0	0	0	323	120	60	[43]
BergerOPLS-DPPC-06[42], ionFF [?]	DPPC	150	72	2880	8	0	8	323	120	60	[44]
BergerOPLS-DPPC-06[42], ionFF [?]	DPPC	1000	72	2778	51	0	51	323	120	60	[45]
CHARMM36[46]	POPC	0	72	2242	0	0	0	303	30	20	[47]
CHARMM36[46], ionFF [?]14.	POPC	350 (NaCl)	72	2085	13	0	13	303	80	60	[48]
CHARMM36[46], ionFF [?]15.	POPC	690 (NaCl)	72	2085	26	0	26	303	73	60	[49]
CHARMM36[46], ionFF [?]	POPC	950 (NaCl)	72	2168	37	0	37	303	80	60	[50]
CHARMM36[46], ionFF [?]	POPC	670 (CaCl$_2$)	72	2164	26	0	52	303	200	120	[51]
MacRog[52]	POPC	0	288	14400	0	0	0	310	90	40	[53]
MacRog[52], ionFF [?]16.	POPC	100 (NaCl)	288	14554	27	0	27	310	90	50	[54]
MacRog[52], ionFF [?]17.	POPC	210 (NaCl)	288	14500	54	0	54	310	90	50	[54]
MacRog[52], ionFF [?]18.	POPC	310 (NaCl)	288	14446	81	0	81	310	90	50	[54]
MacRog[52], ionFF [?]19.	POPC	420 (NaCl)	288	14392	108	0	108	310	90	50	[54]
Orange, ionFF [?]20.	POPC	0	72	2880	0	0	0	298	60	50	?21.
Orange, ionFF [?]	POPC	140 (NaCl)	72	2866	7	0	7	298	120	100	?
Orange, ionFF [?]22.	POPC	510 (NaCl)	72	2802	26	0	26	298	120	100	?23.
Orange, ionFF [?]	POPC	1000 (NaCl)	72	2780	50	0	50	298	120	80	?
Orange, ionFF [?]24.	POPC	510 (CaCl$_2$)	72	2802	0	26	52	298	120	60	? 25.
Slipid[55]	DPPC	0	128	3840	0	0	0	323	150	100	[56]
Slipid[55], ionFF [?]26.	DPPC	150 (NaCl)	600	18000	49	0	49	323	100	40	?
Lipid14/AMBER99SB-ILDN[?]	POPC	0	128	5120	0	0	0	298.15	205	200	[57]
Lipid14/AMBER99SB-ILDN[?]	POPC	150 (NaCl)	128	5120	12	0	12	298.15	205	200	[58]
Lipid14/AMBER99SB-ILDN[?]	POPC	1000 (NaCl)	128	5120	77	0	77	298.15	205	200	[59]
Ulmschneiders/OPLS[?]	POPC	0	128	5120	0	0	0	298.15	205	200	[60]
Ulmschneiders/OPLS[?]	POPC	150 (NaCl)	128	5120	12	0	12	298.15	205	200	[61]
Ulmschneiders/OPLS[?]	POPC	1000 (NaCl)	128	5120	77	0	77	298.15	205	200	[62]

[a] The number of lipid molecules
[b] The number of water molecules
[c] The number of Na^+ molecules
[d] The number of Ca^{2+} molecules
[e] The number of Cl molecules
[f] Simulation temperature
[g] The total simulation time
[h] Time frames used in the analysis

SUPPLEMENTARY INFORMATION

Appendix A: methods

1. Simulated systems

All simulations are ran with a standard setup for planar lipid bilayer in zero tension with periodic boundary conditions with Gromacs software package (version numbers 4.5-X-4.6.X).

2. Simulation details

a. Berger

The simulation without ions is the same as in [31]. The starting structures for simulations with ions is made by replacing water molecules with appropriate amount of ions under study. **31.Samuli, finalize and check the methods.**

The Berger force field was used for the POPC [66], with the dihedral potential next to the double bond taken from [67]. The simulations are identical to previous publications [35, 68, 69]. Timestep of 2 fs was used with leap-frog integrator. Covalent bond lengths were constrained with LINCS algorithm [70, 71]. Coordinates were written every 10 ps. PME with real space cut-off 1.0 nm was used for electrostatics. Plain cut-off was used for the Lennard-Jones interactions with a 1.0 nm cut-off. The neighbour list was updated every 5th step with cut-off 1.0 nm. Temperature was coupled separately for lipids and water to 298 K with the velocity-rescale method [72] with coupling constant 0.1 ps^{-1}. Pressure was semi-isotropically coupled to the athmospheric pressure with the Berendsen method [73].

b. CHARMM36

The simulation without ions is the same as in [31]. The starting structures for simulations with ions is made by replacing water molecules with appropriate amount of ions under study. **32.Samuli, finalize and check the methods.**

Timestep of 1 fs was used with leap-frog integrator. Covalent bonds with hydrogens were constrained with LINCS algorithm [70, 71]. Coordinates were written every 5 ps. PME with real space cut-off 1.4 nm was used for electrostatics. Lennard-Jones interactions were switched to zero between 0.8 nm and 1.2 nm. The neighbour list was updated every 5th step with cut-off 1.4 nm. Temperature was coupled separately for lipids and water to 303 K with the velocity-rescale method [72] with coupling constant 0.2 ps. Pressure was semi-isotropically coupled to the athmospheric pressure with the Berendsen method [73].

c. MacRog

The simulation parameters are identical to those employed in our earlier study [31] for the full hydration and dehydration simulations. The initial structures with varying amounts of NaCl were constructed from an extensively hydrated bilayer by replacing water molecules with ions using the Gromacs tool genion. Even at the highest considered salt concentration, the amount of water molecules per lipid after this replacement process was still greater than 50.

d. Orange

33.Jukka Maatta and Luca Monticelli, please deliver as much details as you can.

e. Slipids

The simulation without ions is the same as in [31]. **34.Add references to Slipids with ions.** For the simulations with ions, the starting DPPC lipid bilayer, which was built with the online CHARMM-GUI (http://www.charmm-gui.org/), contained 600 lipids, 30 water molecules/lipid, Na$^+$ and Cl$^-$ ions (150 mM NaCl). The TIP3P water model was used to solvate the system. All-atom MD simulations of DPPC lipid bilayers were performed at ten different temperatures (283, 298, 303, 308, 312, 313, 314, 318, 323, and 333 K) using the GROMACS software package version 4.5.5 and the Stockholm lipids (Slipids) force field parameters for phospholipids. After energy minimization and a short equilibration run of 50 ps (time step 1 fs), 100 ns production runs were performed using a time step of 2 fs with leap-frog integrator. All covalent bonds were constrained with the LINCS algorithm. Coordinates were written every 100 ps. PME with real space cut-off at 1.0 nm was used for Coulomb interactions. Lennard-Jones interactions were switched to zero between 1.0 nm and 1.4 nm. The neighbour lists were updated every 10$^{\text{th}}$ step with a cut-off of 1.6 nm. Temperature was coupled separately for upper and bottom leaflets of the lipid bilayer, and for water to one of the temperatures reported above with the Nosé-Hoover thermostat using a time constant of 0.5 ps. Pressure was semi-isotropically coupled to the atmospheric pressure with the Parrinello-Rahman barostat using a time constant of 10 ps. The last 40 ns of each simulation was employed for the analysis of DPPC choline and glycerol backbone order parameters.

3. Analysis

The order parameters were calculated from simulation trajectories directly applying the equation $S_{\text{CH}} = \langle \frac{3}{2} \cos^2 \theta - \frac{1}{2} \rangle$, where θ is the angle between a given C–H bond and the bilayer normal. For united atom models the hydrogen locations were regenerated for each molecule in each frame after the simulation trajectory was created. ??The statistical error estimate for each order parameter calculated from simulation was roughly 0.01, which is much smaller than the differences discussed in this work.?? **35.Markus: What do the question marks mean? Was the error estimation not performed yet?**

4. Effect of ion model and polarization

We also tested if different ion models and implicit accounting of polarization would affect ion binding. Changing the model description from Berger-DPPC-98 [?] and Gromos ion parameters [?]**36.** to OPLS-AA compatible Berger-DPPC-06 [42] and Åqvist ions [74] results in slightly decreased ion binding affinity as seen from the density plots in Figure 6 [75, 76]. The failure of Gromos ions to properly account ion–ion and ion–water binding propensities of Na$^+$ and Cl$^-$ ions has been reported previously [77]. The Åqvist ions have been parameterized in aqueous solutions with good agreement to experimental energies [74]. Yet, the binding affinity of ions

to lipid bilayers has not been calibrated—instead it is assumed to work based purely on forces obtained using combination rules. Compared to Gromos ions, Åqvist parameters are better, yet Na^+ overbinding still occurs.

To account for polarization effects in non-polarizable models, Leontyev et al. [65] have suggested that ion charges should be scaled by a factor of 0.7. We scaled the charges of both Gromos and Åqvist ions. After scaling, both the order parameter changes due to ions and the ion affinity into a bilayer are decreased in both ion models, see Figs. 5, 6 and 7 [78, 79]. The intuitive explanation is that by scaling the partial charges the charge discrepancy between the ion and water partial charges is decreased. This means that there is a lesser driving force for ions to bind to the highly-charged phosphate group. Furthermore, with Berger-DPPC-06 and scaled Åqvist ions (Q=0.7) we obtain that there is only very weak binding of sodium to DPPC as observed experimentally (right side of Figure 7). In scaled models the order parameter changes are

also small. However, the ion concentration is also small. To be fully conclusive, if the affinity can be fixed by scaling, we need to run simulations also with large concentrations.

The results indicate that the polarization effect actually improves ion binding affinities irrespectively of the model. However, the drawback of the scaled charges is that the total charge of the simulation box is non-zero whenever counterions and charged molecules are present. This may cause simulation artefacts. Even though in methods such as PME the residual charge does not affect the forces (and thus dynamics), it still has an effect to the energies. This is because the potential from the residual charge is 'smeared in the box' and so depends on the possibly fluctuating (at least in NPT conditions) volume of the simulation box.

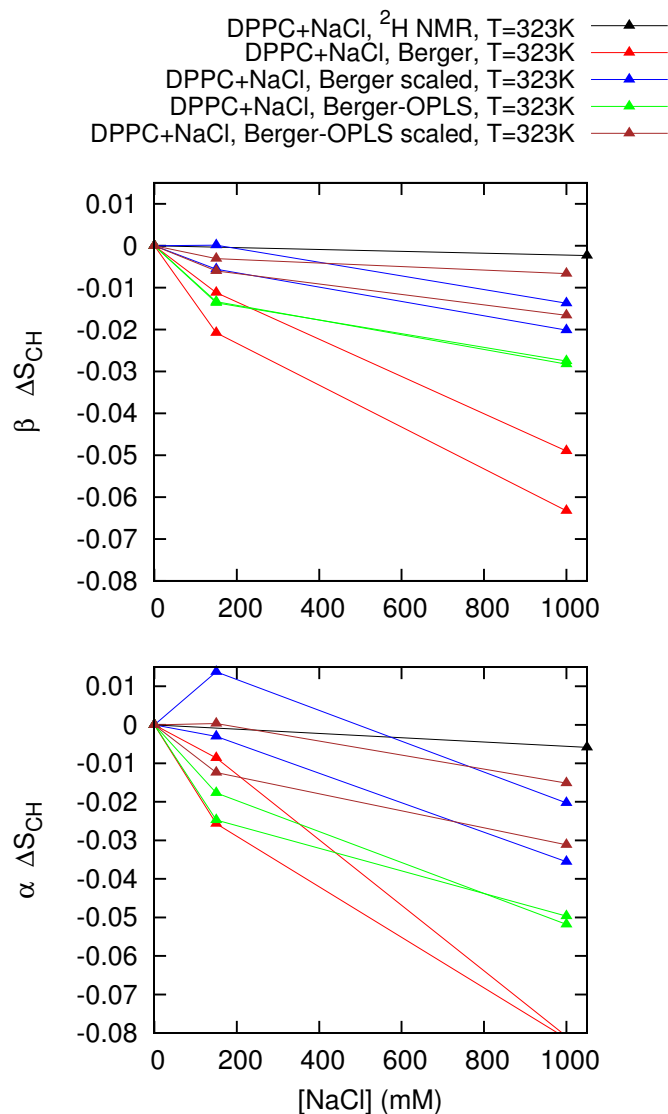## 5. Structural changes induced by $CaCl_2$

TODO

FIG. 5: Order parameter changes in scaled and non-scaled models. The Berger-OPLS compatible model results are missing since there are no results without ions for this.
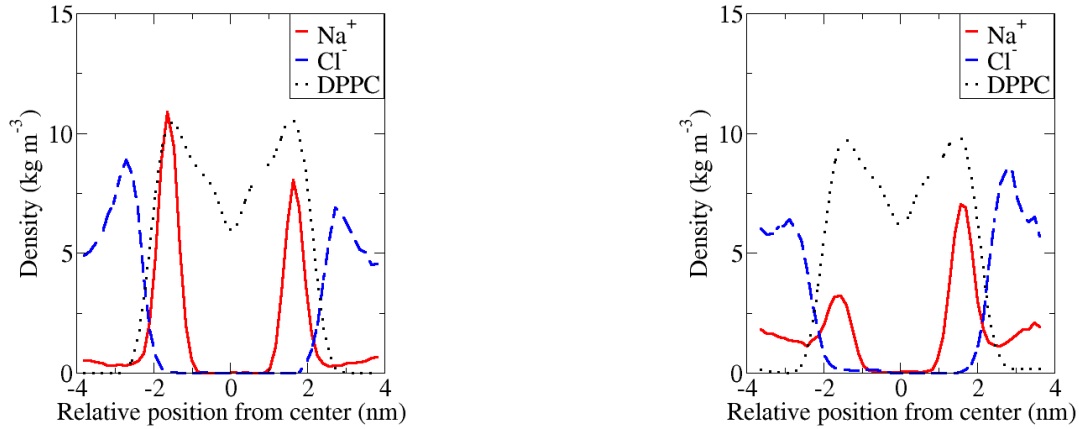
FIG. 6: Density plots of DPPC bilayer and ions. DPPC density has been scaled down by a factor of 100 for clarity. Left: Berger-DPPC-98 model with Gromos ions. Right: Berger-DPPC-06 model with Åqvist ions.
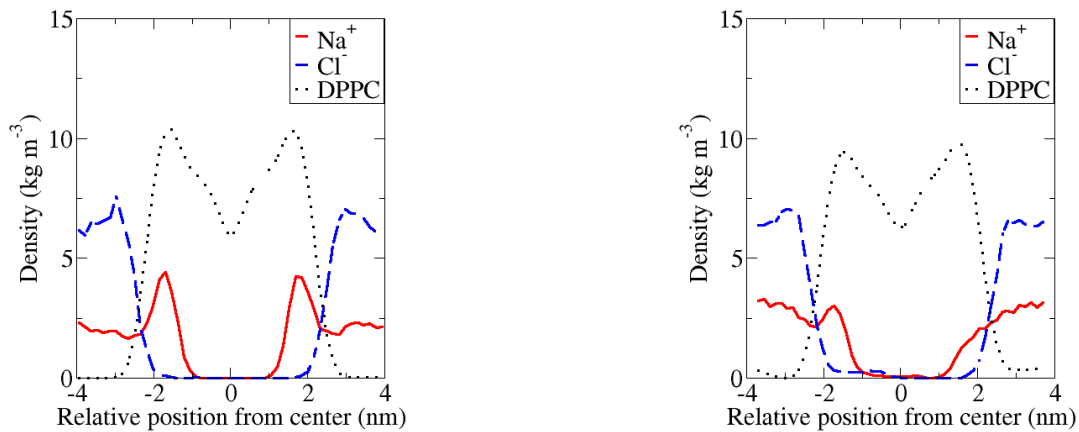

FIG. 7: Density plots of DPPC bilayer and polarization corrected ions, where ion charges are scaled by 0.7. DPPC density has been scaled down by a factor of 100 for clarity. Left: Berger-DPPC-98 model with scaled Gromos ions. Right: Berger-DPPC-06 model with scaled Åqvist ions.

FIG. 8: Dihedral angle distributions for O-β-α-N dihedral with different CaCl$_2$ concentrations.

[1] M. Eisenberg, T. Gresalfi, T. Riccio, and S. McLaughlin, Biochemistry **18**, 5213 (1979).

[2] G. Cevc, Biochim. Biophys. Acta - Rev. Biomemb. **1031**, 311 (1990).

[3] J.-F. Tocanne and J. Teissi, Biochimica et Biophysica Acta (BBA) - Reviews on Biomembranes **1031**, 111 (1990).

[4] H. Binder and O. Zschörnig, Chem. Phys. Lipids **115**, 39 (2002).

[5] J. J. Garcia-Celma, L. Hatahet, W. Kunz, and K. Fendler, Langmuir **23**, 10074 (2007).

[6] E. Leontidis and A. Aroti, The Journal of Physical Chemistry B **113**, 1460 (2009).

[7] R. Vacha, S. W. I. Siu, M. Petrov, R. A. Böckmann, J. Barucha-Kraszewska, P. Jurkiewicz, M. Hof, M. L. Berkowitz, and P. Jungwirth, J. Phys. Chem. A **113**, 7235 (2009).

[8] B. Klasczyk, V. Knecht, R. Lipowsky, and R. Dimova, Langmuir **26**, 18951 (2010).

[9] F. F. Harb and B. Tinland, Langmuir **29**, 5540 (2013).

[10] G. Pabst, A. Hodzic, J. Strancar, S. Danner, M. Rappolt, and P. Laggner, Biophys. J. **93**, 2688 (2007).

[11] A. Filippov, G. Ordd, and G. Lindblom, Chemistry and Physics of Lipids **159**, 81 (2009).

[12] R. A. Böckmann, A. Hac, T. Heimburg, and H. Grubmüller, Biophys. J. **85**, 1647 (2003).

[13] R. A. Böckmann and H. Grubmüller, Ang. Chem. Int. Ed. **43**, 1021 (2004).

[14] S. Garcia-Manyes, G. Oncins, and F. Sanz, Biophys. J. **89**, 1812 (2005).

[15] S. Garcia-Manyes, G. Oncins, and F. Sanz, Electrochimica Acta **51**, 5029 (2006), ISSN 0013-4686, bioelectrochemistry 2005 Bioelectrochemistry 2005, URL http://www.sciencedirect.com/science/article/pii/S0013468606002775.

[16] T. Fukuma, M. J. Higgins, and S. P. Jarvis, Phys. Rev. Lett. **98**, 106101 (2007).

[17] U. Ferber, G. Kaggwa, and S. Jarvis, European Biophysics Journal **40**, 329 (2011), ISSN 0175-7571, URL http://dx.doi.org/10.1007/s00249-010-0650-7.

[18] L. Redondo-Morata, G. Oncins, and F. Sanz, Biophysical Journal **102**, 66 (2012).

[19] H. Akutsu and J. Seelig, Biochemistry **20**, 7366 (1981).

[20] C. Altenbach and J. Seelig, Biochemistry **23**, 3913 (1984).

[21] J. Seelig, P. M. MacDonald, and P. G. Scherer, Biochemistry **26**, 7535 (1987).

[22] P. G. Scherer and J. Seelig, Biochemistry **28**, 7720 (1989).

[23] S. A. TATULIAN, European Journal of Biochemistry **170**, 413 (1987), ISSN 1432-1033, URL http://dx.doi.org/10.1111/j.1432-1033.1987.tb13715.x.

[24] R. J. Clarke and C. Lpfert, Biophysical Journal **76**, 2614 (1999).

[25] M. L. Berkowitz, D. L. Bostick, and S. Pandit, Chem. Rev. **106**, 1527 (2006).

[26] V. Knecht and B. Klasczyk, Biophys. J. **104**, 818 (2013).

[27] J. N. Sachs, H. Nanda, H. I. Petrache, and T. B. Woolf, Biophys. J. **86**, 3772 (2004).

[28] A. Cordomi, O. Edholm, and J. J. Perez, J. Chem. Theo. Comput. **5**, 2125 (2009).

[29] C. Valley, J. Perlmutter, A. Braun, and J. Sachs, J. Membr. Biol. **244**, 35 (2011).

[30] M. L. Berkowitz and R. Vacha, Acc. Chem. Res. **45**, 74 (2012).

[31] A. Botan, A. Catte, F. Favela, P. Fuchs, M. Javanainen, W. Kulig, A. Lamberg, M. S. Miettinen, L. Monticelli, J. Määttä, et al., *To-*

wards atomistic resolution structure of phosphatidylcholine glycerol backbone and choline headgroup at different ambient conditions, http://arxiv.org/abs/1309.2131v2 (2015), nMRlipids project, nmrlipids.blogspot.fi, 1309.2131.

[32] M. Hong, K. Schmidt-Rohr, and A. Pines, Journal of the American Chemical Society **117**, 3310 (1995).

[33] M. Hong, K. Schmidt-Rohr, and D. Nanz, Biophysical Journal **69**, 1939 (1995).

[34] J. D. Gross, D. E. Warschawski, and R. G. Griffin, Journal of the American Chemical Society **119**, 796 (1997).

[35] S. Ollila, M. T. Hyvönen, and I. Vattulainen, J. Phys. Chem. B **111**, 3139 (2007).

[36] O. H. S. Ollila, T. Ferreira, and D. Topgaard (2014), URL {http://dx.doi.org/10.5281/zenodo.13279}.

[37] O. O. H. Samuli, *MD simulation trajectory and related files for POPC bilayer with 340mM NaCl (Berger model delivered by Tieleman, ffgmx ions, Gromacs 4.5)* (2015), URL http://dx.doi.org/10.5281/zenodo.32144.

[38] O. O. H. Samuli, *MD simulation trajectory and related files for POPC bilayer with 340mM CaCl_2 (Berger model delivered by Tieleman, ffgmx ions, Gromacs 4.5)* (2015), URL http://dx.doi.org/10.5281/zenodo.32173.

[39] S.-J. Marrink, O. Berger, P. Tieleman, and F. Jähnig, Biophysical Journal **74**, 931 (1998).

[40] J. Määttä (2015), URL {http://dx.doi.org/10.5281/zenodo.13934}.

[41] J. Määttä, *Dppc_berger_nacl_1mol* (2015), URL http://dx.doi.org/10.5281/zenodo.17210.

[42] D. P. Tieleman, J. L. MacCallum, W. L. Ash, C. Kandt, Z. Xu, and L. Monticelli, J. Phys. Condens. Matter **18**, S1221 (2006).

[43] J. Määttä, *Dppc_berger_opls06* (2015), URL http://dx.doi.org/10.5281/zenodo.17237.

[44] J. Määttä, *Dppc_berger_opls06_nacl* (2015), URL http://dx.doi.org/10.5281/zenodo.16484.

[45] J. Määttä, *Dppc_berger_opls06_nacl_1mol* (2015), URL http://dx.doi.org/10.5281/zenodo.17208.

[46] J. B. Klauda, R. M. Venable, J. A. Freites, J. W. O'Connor, D. J. Tobias, C. Mondragon-Ramirez, I. Vorobyov, A. D. M. Jr, and R. W. Pastor, J. Phys. Chem. B **114**, 7830 (2010).

[47] O. O. H. Samuli and M. Miettinen (2015), URL {http://dx.doi.org/10.5281/zenodo.13944}.

[48] S. Ollila, *MD simulation trajectory and related files for POPC bilayer with 350mM NaCl (CHARMM36, Gromacs 4.5)* (2015), URL http://dx.doi.org/10.5281/zenodo.32496.

[49] S. Ollila, *MD simulation trajectory and related files for POPC bilayer with 690mM NaCl (CHARMM36, Gromacs 4.5)* (2015), URL http://dx.doi.org/10.5281/zenodo.32497.

[50] S. Ollila, *MD simulation trajectory and related files for POPC bilayer with 950mM NaCl (CHARMM36, Gromacs 4.5)* (2015), URL http://dx.doi.org/10.5281/zenodo.32498.

[51] S. Ollila, *MD simulation trajectory and related files for POPC bilayer with 670mM CaCl_2 (CHARMM36, Gromacs 4.5)* (2015), URL http://dx.doi.org/10.5281/zenodo.32570.

[52] A. Maciejewski, M. Pasenkiewicz-Gierula, O. Cramariuc, I. Vattulainen, and T. Rog, The Journal of Physical Chemistry B **118**, 4571 (2014).

[53] M. Javanainen (2014), URL {http://dx.doi.org/10.5281/zenodo.13498}.

[54] M. Javanainen, *POPC @ 310K, varying amounts of NaCl. Model by Maciejewski and Rog* (2015), URL http://dx.doi.org/10.5281/zenodo.14976.

[55] J. P. M. Jämbeck and A. P. Lyubartsev, The Journal of Physical Chemistry B **116**, 3164 (2012).

[56] J. Määttä (2014), URL {http://dx.doi.org/10.5281/zenodo.13287}.

[57] M. Girych and O. H. S. Ollila, *Popc_amber_lipid14_verlet* (2015), URL http://dx.doi.org/10.5281/zenodo.30898.

[58] M. Girych and O. H. S. Ollila, *Popc_amber_lipid14_nacl_015mol* (2015), URL http://dx.doi.org/10.5281/zenodo.30891.

[59] M. Girych and O. H. S. Ollila, *Popc_amber_lipid14_nacl_1mol* (2015), URL http://dx.doi.org/10.5281/zenodo.30865.

[60] M. Girych and O. H. S. Ollila, *Popc_ulmschneider_opls_verlet_group* (2015), URL http://dx.doi.org/10.5281/zenodo.30904.

[61] M. Girych and O. H. S. Ollila, *Popc_ulmschneider_opls_nacl_015mol* (2015), URL http://dx.doi.org/10.5281/zenodo.30892.

[62] M. Girych and O. H. S. Ollila, *Popc_ulmschneider_opls_nacl_1mol* (2015), URL http://dx.doi.org/10.5281/zenodo.30894.

[63] H. Hauser, M. C. Phillips, B. Levine, and R. Williams, Nature **261**, 390 (1976).

[64] H. Hauser, W. Guyer, B. Levine, P. Skrabal, and R. Williams, Biochimica et Biophysica Acta (BBA) - Biomembranes **508**, 450 (1978), ISSN 0005-2736, URL http://www.sciencedirect.com/science/article/pii/0005273678900913.

[65] I. Leontyev and A. Stuchebrukhov, Phys. Chem. Chem. Phys. **13**, 2613 (2011).

[66] O. Berger, O. Edholm, and F. Jähnig, Biophys. J. **72**, 2002 (1997).

[67] M. Bachar, P. Brunelle, D. P. Tieleman, and A. Rauk, J. Phys. Chem. B **108**, 7170 (2004).

[68] T. M. Ferreira, F. Coreta-Gomes, O. H. S. Ollila, M. J. Moreno, W. L. C. Vaz, and D. Topgaard, Phys. Chem. Chem. Phys. **15**, 1976 (2013).

[69] T. M. Ferreira, O. H. S. Ollila, R. Pigliapochi, A. P. Dabkowska, and D. Topgaard, The Journal of Chemical Physics **142**, 044905 (2015), URL http://scitation.aip.org/content/aip/journal/jcp/142/4/10.1063/1.4906274.

[70] B. Hess, H. Bekker, H. J. C. Berendsen, and J. G. E. M. Fraaije, J. Comput. Chem. **18**, 1463 (1997).

[71] B. Hess, Journal of Chemical Theory and Computation **4**, 116 (2008).

[72] G. Bussi, D. Donadio, and M. Parrinello, The Journal of Chemical Physics **126** (2007).

[73] H. J. C. Berendsen, J. P. M. Postma, W. F. van Gunsteren, A. DiNola, and J. R. Haak, J. Chem. Phys. **81**, 3684 (1984).

[74] J. Aaqvist, The Journal of Physical Chemistry **94**, 8021 (1990), http://dx.doi.org/10.1021/j100384a009, URL http://dx.doi.org/10.1021/j100384a009.

[75] J. Määttä (2015), URL {http://dx.doi.org/10.5281/zenodo.16319}.

[76] J. Määttä (2015), URL {http://dx.doi.org/10.5281/zenodo.16484}.

[77] M. M. Reif, M. Winger, and C. Oostenbrink, Journal of Chemical Theory and Computation **9**, 1247 (2013), pMID: 23418406,

http://dx.doi.org/10.1021/ct300874c, URL `http://dx.doi.org/10.1021/ct300874c`.

[78] J. Määttä (2015), URL `{http://dx.doi.org/10.5281/zenodo.16320}`.

[79] J. Määttä (2015), URL `{http://dx.doi.org/10.5281/zenodo.16485}`.